Experimental Procedure and Hardening Model for Simulation Considering Forming and Baking Effects

JiHo Lim[1], Haea Lee[1], Jisik Choi[1]

[1]POSCO

1 Introduction

The automotive body is manufactured by assembling parts made by forming, and then going through a painting process. Sheet metal parts formed by press have the plastic strain, and bake hardening that material strength increases according to the plastic strain during the baking process of painting, occurs. Therefore, the actual assembled automotive parts are stronger than the original materials due to the combined effects of work hardening and bake hardening. Automobile crash analysis generally applies the properties of the original material, but the change of material properties in real parts acts as a factor of error in crash analysis. Especially, these characteristic is more pronounced in giga-steel. Considering the increasing trend of giga-steel for weight reduction, it is necessary to consider the change of material properties due to work hardening and bake hardening in crash analysis.

In order to consider the material properties due to the pre-strain and baking in the crash simulation, it is necessary to derive the stress-strain curve after maximum load. Generally, the stress-strain curve after the maximum load cannot be directly calculated using formulas from experimental data, so, indirect methods are used. Since the bulge test can obtain the stress-strain curve up to larger strain than the tensile test, the bulge test can be used to convert the stress-strain curve into tensile stress-strain curve based on the principle of equivalent plastic work. Stoughton et al. [1] used a method to obtain the stress-strain curve through numerical analysis in the relationship between true stress and strain on the surface of a tensile specimen by the DIC system. This method has limitations that the strain is uniform in the width direction of the specimen and the difference between the stress in longitudinal direction and the von Mises stress is not large.

Many researchers have studied to consider the bake hardening effect in the simulation. Koch et al. [2] and Riemensperger [3] applied the method of shifting the work hardening curve by the increase in strength due to bake hardening in the simulation. Thuillier et al. [4] proposed an empirical work hardening model that expresses the yield function as the sum of the stress of the base material and overstress due to baking. Schwab [5] et al. explained that the upper yield point generated by yield point elongation is larger than the observed value and the lower yield point is smaller than the observed value. Ballarin et al. [6] proposed a formula expressing bake hardening as the sum of the Cottrel effect and the precipitation effect. Durrenbergera et al. [7] proposed a material model according to pre-strain and bake hardening, and verified the analysis applying the material model with an axial test of a hat specimen.

This paper aims to develop a test method and simulation technique to consider the work hardening and baking hardening effects according to the forming history in the crash analysis. A testing method was developed to suppress the fracture in the curvature of the tensile specimen, and a DIC inverse method was developed to obtain the stress-strain curve after the maximum load even for non-uniform strain distribution using the strain obtained from the DIC system. In order to apply the material properties obtained in the experiment to the simulation, novel work hardening model considering work hardening and bake hardening was developed and verified by LS-Dyna user material subroutine.

2 Tensile properties after baking according to the pre-strain

2.1 Test method for bake hardening property

In standard, bake hardening index is defined as the increase of material strength at the pre-strain after baking a pre-strained specimen and then re-tensioning it. The baking condition is heating at 170℃ for 20 minutes. Since the bake hardening test is generally re-tensioned with the same specimen after baking, a difference in bake hardening occurs due to non-uniform strain distribution in the curvature. Giga-steel is more affected by the phenomenon, and fracture may occur outside the gauge section as shown in Fig. 1. When this happens, it is impossible to obtain the stress-strain curve as shown in Fig. 2 since the strain is not measured in a extensometer. In general, as the pre-strain increases, the material strength after baking increases. When baking after applying the pre-strain to the tensile specimen, the material strength of the grip and the curvature part is lowered compared to the gage section. If tension is applied here as it is, strain is concentrated at the starting point of the curvature and fracture occurs.

In this paper, in order to eliminate the non-uniformity of material strength after baking, as shown in Fig. 3, pre-deformation was applied to a KS-1B specimen with a parallel length of 220 mm, and a ASTM tensile specimen re-machined in parallel part of KS-1B specimen was re-tensioned. When done this way, the fracture of the curvature part was significantly improved in the material with tensile strength up to 1180 MPa.

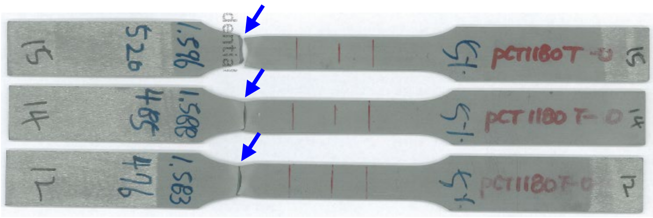

Fig.1: Deformed shape after failure of ASTM specimens of 1180TRIP with 5% pre-strain and baking

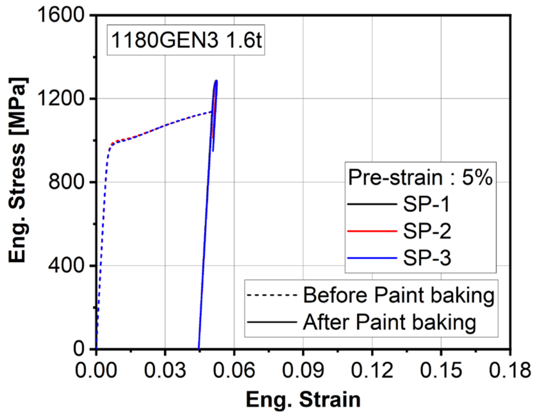

Fig.2: Engineering stress-strain curves of ASTM specimens with 5% pre-strain and baking

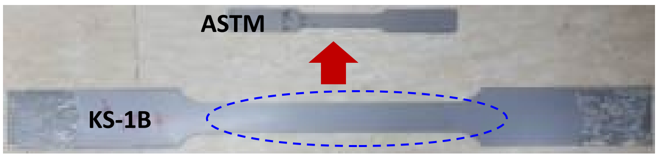

Fig.3: ASTM specimen re-machined from KS-1B specimen with pre-strain and baking

2.2 Calculation of strain and stress considering pre-strain

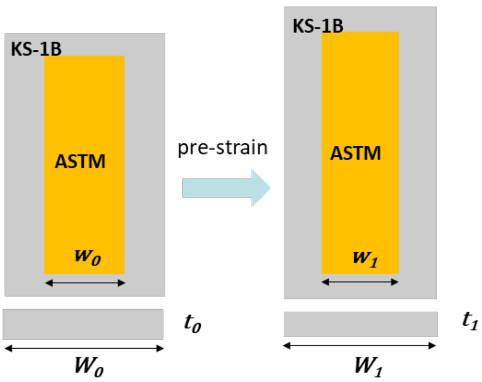

Fig.4: Schematic diagram of shapes of KS-1B and ASTM specimens before and after pre-deformation

To calculate the stress after a test, the force is divided by the cross-sectional area of the specimen based on initial dimensions before pre-deformation. However, since the testing method in this paper is re-machining the specimen after pre-deformation, it is not possible to directly measure the width of the re-machined ASTM tensile specimen before pre-deformation. It can be assumed that the specimen is deformed at the same rate in the width and thickness direction. Therefore, the width of the re-machined specimen before pre-deformation in Fig. 4 can be calculated with a simple proportional formula as shown in equation (1).

$$\boldsymbol{A_{initial\_ASTM}} = w_0 \times t_0 = (\boldsymbol{w_1} \times \frac{\boldsymbol{w_0}}{\boldsymbol{w_1}}) \times \boldsymbol{t_0} \tag{1}$$

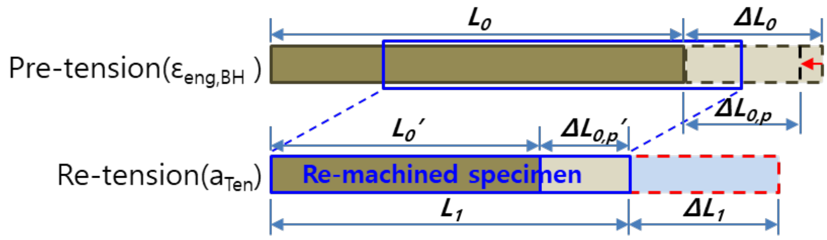

Fig.5: Schematic diagram for the variation of gauge section length after pre tension

The strain measured by the DIC system in the tensile test of the re-machined ASTM specimen is the value calculated as the strain of 0 for the re-machined specimen after pre-deformation. Therefore, it is necessary to analyze the relationship between the total strain and the strain measured by DIC, and adjust the strain based on the original state without pre-deformation.

The plastic strain after removing the pre-deformation load (ε_{BH}^{p}) is calculated as the engineering strain of pre-deformation ($\varepsilon_{eng,BH}$) and the engineering stress (S_{BH}) as shown in Equation (2). And engineering strain after removing the pre-deformation load ($\varepsilon_{eng,BH}^{p}$) is calculated by equation (3). In addition, the gauge length of the pre-deformed specimen (L_0), length change due to pre-deformation (ΔL_0), length change after pre-deformation and elastic recovery ($\Delta L_{0,p}$), the gage length of the re-machined specimen (L_1), the gauge length of the re-machined specimen before pre-deformation (L_0') and the permanant deformation length of the re-machined specimen ($\Delta L_{o,p}'$) have the relationship as Equations (4) and (5).

$$\varepsilon_{BH}^{p} = \varepsilon_{BH} - \frac{\sigma_{BH}}{E} = \varepsilon_{BH} - \frac{S_{BH}e^{\varepsilon_{BH} - \frac{1-2\nu}{E}\sigma_{BH}}}{E} \approx ln\,(1 + \varepsilon_{eng,BH}) - \frac{S_{BH}(1+\varepsilon_{eng,BH})}{E} \tag{2}$$

$$\varepsilon_{eng,BH}^{p} = e^{\varepsilon_{BH}^{p}} - 1 = \left(1 + \varepsilon_{eng,BH}\right)e^{-\frac{S_{BH}\left(1+\varepsilon_{eng,BH}\right)}{E}} - 1 \tag{3}$$

$$\varepsilon_{eng,BH}^{p} = \frac{\Delta L_{0,p}}{L_0} = \frac{\Delta L_{0,p}'}{L_0'} \tag{4}$$

$$L_0' = \frac{L_1}{L_0 + \Delta L_{0,p}} L_0 \tag{5}$$

The strain (ε_m) measured by the DIC system in the re-tension of the re-machined specimen is expressed as equation (6).

$$\varepsilon_m = \ln\,(1 + \frac{\Delta L_1}{L_1}) \tag{6}$$

The engineering strain ($\varepsilon_{eng,T}$) for the state before pre-deformation is expressed by equation (7). Substituting equaton (4) and (5) in to equation (7) gives equation (8). Substituting equation (6) into equation (8) produces equation (9). And the true strain (ε_T) for the state before pre-deformaton is expressed as equation (10). In addition, the stress(σ) based on pre-deformation state is expressed by equation (11).

$$\varepsilon_{eng,T} = \frac{\Delta L_{0,p'}}{L_0'} + \frac{\Delta L_1}{L_0'} \tag{7}$$

$$\varepsilon_{eng,T} = \varepsilon^{p}_{eng,BH} + \frac{\Delta L_1}{\frac{L_1}{L_0+\Delta L_{0,p}} L_0} = \varepsilon^{p}_{eng,BH} + \left(1 + \varepsilon^{p}_{eng,BH}\right)\frac{\Delta L_1}{L_1} \tag{8}$$

$$\varepsilon_{eng,T} = \left(1 + \varepsilon_{eng,BH}\right) e^{-\frac{S_{BH}\left(1+\varepsilon_{eng,BH}\right)}{E}} e^{\varepsilon_m} - 1 \tag{9}$$

$$\varepsilon_T = \ln\left(\varepsilon_{eng,T} + 1\right) = \varepsilon_{BH} - \frac{S_{BH}\left(1+\varepsilon_{eng,BH}\right)}{E} + \varepsilon_m \tag{10}$$

$$\sigma = S e^{\varepsilon_T} = S e^{\varepsilon_{BH} - \frac{S\left(1+\varepsilon_{eng,BH}\right)}{E} + \varepsilon_m} \tag{11}$$

2.3 Results of tensile tests

Tensile tests were performed after pre-deformation and baking for 590DP and 980DP steels, and the engineering stress-strain curves were obtained as shown in Fig. 6. Stress-strain curves of 590DP steel with respect to the pre-strain shift upper without changing the shape of curve. In 980DP steel, the strength of the material increases as the yield point elongation occurs up to 2% of the pre-strain. On the other hand, for the pre-strain of 3% or more, the upper yield point becomes the maximum stress, and the stress continuously decreases after the upper yield point. Overall, there is a tendency for the maximum stress to increase as the pre-strain increases.

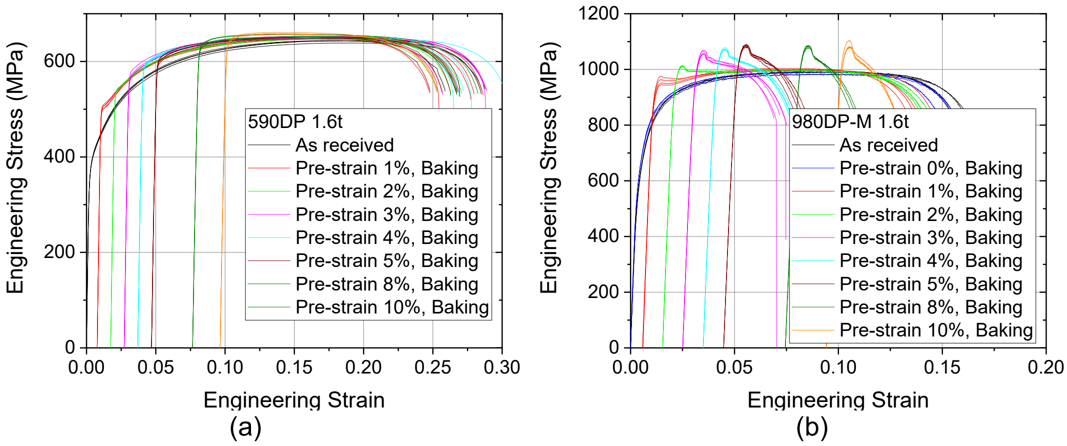

Fig.6: Engineering stress-strain curves after baking according to pre-strain: (a) 590DP; (b) 980DP

Fig. 7 shows the strain distribution before fracture according to the pre-strain of 980DP. Necking is observed up to 5% of the pre-strain, but as the pre-strain increases, the deformation before fracture tends to concentrate in an oblique line. In particular, when the pre-strain is 8% or more, necking is not observed and shear band fracture occurs. In general, Lüders band propagates to the gauge section during yield point elongation, and necking and fracture occurs through work hardening zone and ultimate strength. However, when the upper yield point becomes equal to the maximum stress after baking as the pre-strain increases, the first Lüders band does not propagate and the deformation concentrates, resulting in shear band fracture.

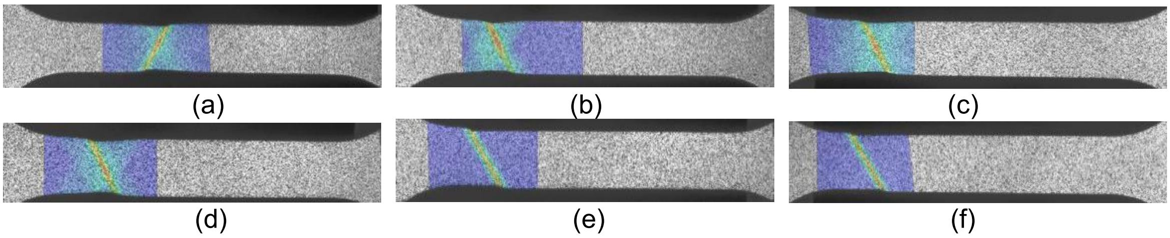

Fig.7: Strain distribution of 980DP steel before fracture with respect to the pre-strain: (a) as received; (b) 2%; (c) 4%; (d) 5%; (e) 8%; (f) 10%

Fig. 8 shows the changes in tensile strength according to the pre-strain. In 590DP steel, the tensile strength gradually increases, and the increase for the pre-strain of 10% is around 20MPa. In 980DP, there is no change in tensile strength when baking without pre-strain, but the tensile strength increases gradually up to the pre-strain of 2% and then rapidly increases up to the pre-strain of 4%. The tensile strength for over the pre-strain of 4% maintains an almost constant value, and the increase in tensile strength is about 90MPa, which can sufficiently affect the crash performance of the material.

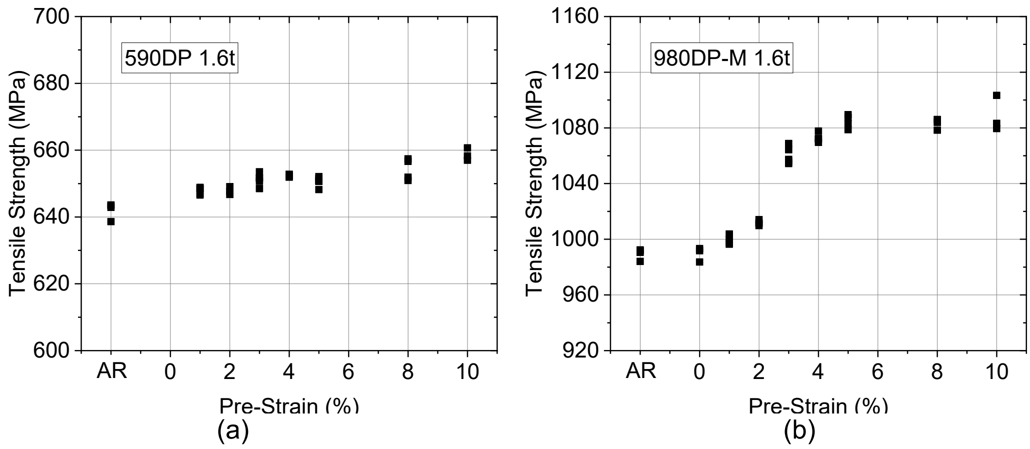

Fig.8: Tensile strength according to pre-strain: (a) 590DP; (b) 980DP

3 Calculation of true stress-strain curves

3.1 DIC inverse method for true stress-strain curve over maximum load

It was confirmed that the strength of the material generally increased after baking with pre-strain. Especially, the increase in material strength of giga-steel can have a significant effect on the crash performance. Therefore, the change of material properties by forming and baking should be considered in order to enhance the accuracy of crash simulation. The stress-strain curve is required at the crash simulation, so engineering stress-strain curve in Fig. 6 should be converted to true stress-strain curves. However, when the upper yield point is equal to the ultimate strength as in 980DP steel, there is no way to calculate the true stress-strain curve by formulas.

In this paper, it was developed the DIC inverse method which obtains the stress-strain curves after the maximum load from numerical optimization by comparing the force calculated from the strain measured in DIC system with the load-displacement curve. As shown in Fig. 9, the sum of forces (f_i) in the small lattice of any cross-section and the force (F) measured in the testing machine are always the same. If the relationship between stress and strain of a material is known, the force (f_i) of the small lattice can be calculated from the strain measured by the DIC system. However, it is not possible to directly calculate the force (f_i) of the small lattice because the stress-strain curve is the what is desired to be obtained in the experiment. In first, an arbitrary stress-strain curve is assumed, and the stress-strain curves is optimized so that the sum of the calculated forces (Σf_i) and the force (F) measured by the testing equipment are equal.

Assuming the blue graph in Fig. 10 as the initial stress-strain curve, the calculated sum of forces (Σf_i) shown in the blue graph of Figure 11 is vastly different from the black load graph obtained in the experiment. When performing optimization using in-house optimization program using Excel VBA, the sum of calculated forces was matched precisely with the load-displacement curve in the experiment as shown in the red graph of Fig. 11. The final output as the stress-strain curve is the red graph of Fig. 10.

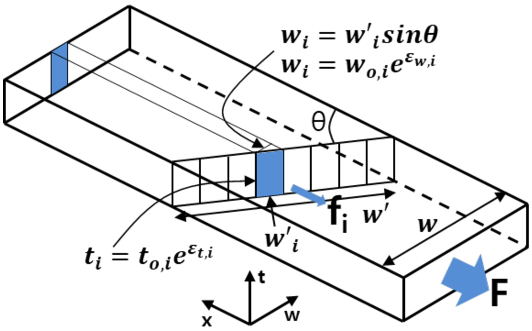

Fig.9: Schematic diagram of an arbitrary cross section in the parallel section of a tensile specimen

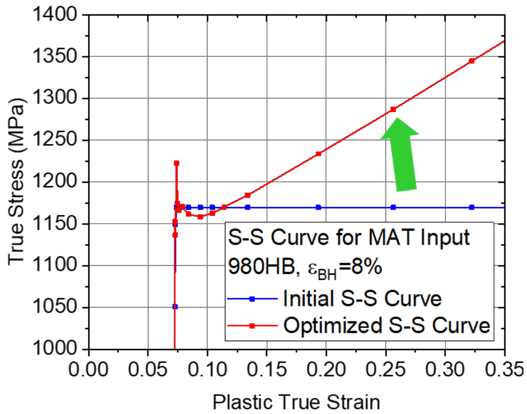

Fig.10: Initial input and optimized stress-strain curves by DIC inverse method

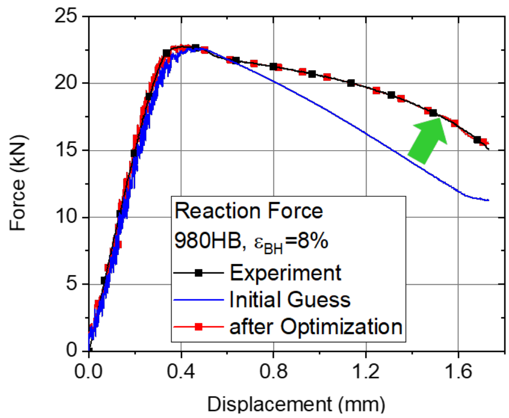

Fig.11: Comparison of force-displacement curves between experiment and DIC inverse method

The stress obtained by the DIC inverse method is the stress in the tensile direction (σ_x), but the stress in stress-strain curve is the Von Mises stress. If the two stresses differ, the DIC inverse method can no longer be used. Fig. As shown in Fig. 12, the simulation of tensile test was performed on a quarter model of the tensile specimen, and the difference between σ_x and σ_{VM} was examined. As shown in the strain distribution in Fig. 13, necking occurs in parallel section after ultimate strength, and the strain distribution becomes non-uniform in the width direction.

The changes in σ_x and σ_{VM} between the center and the edge are shown in Fig. 14. When the deformation is the transverse direction becomes non-uniform after ultimate strength, the difference between σ_x and σ_{VM} occurs. Therefore, it should be considered that the error of the DIC inverse method also increases when local necking occurs. Nevertheless, reliable stress-strain curves can still be obtained by the DIC inverse method in a range of strain that is 2 to 30 time higher than the uniform elongation. Especially, there is an advantage in obtaining stress-strain curves even for cases where uniform elongation is nothing such in shear band fracture.

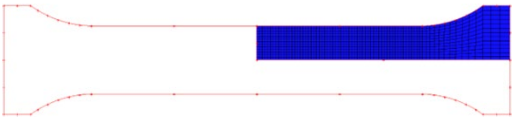

Fig.12: 1/4 model of a tensile specimen

Fig.13: Variation of strain contour after necking

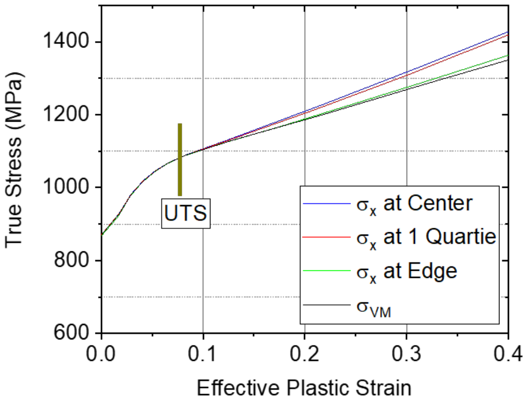

Fig.14: Variation of σ_x and Von-Mises stress

3.2 True stress-strain curves of steels

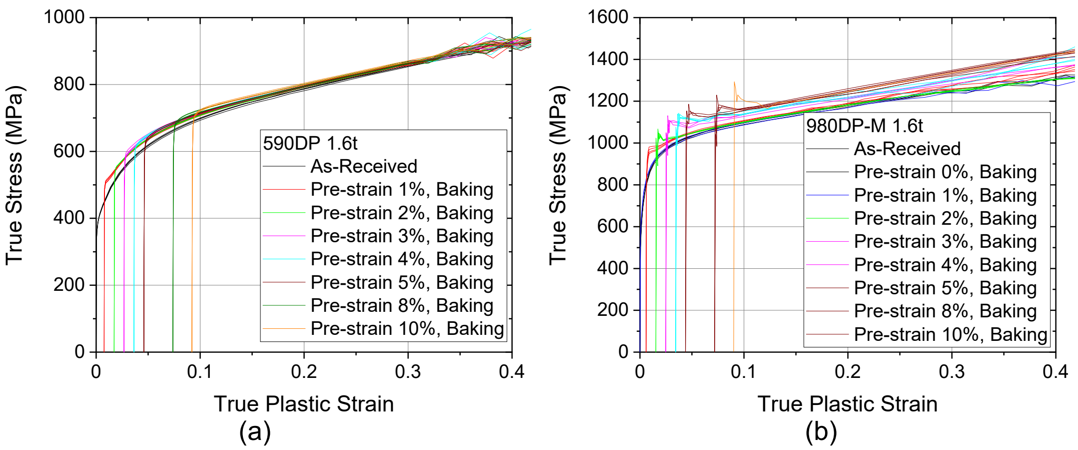

Fig.15: True stress-strain curves after baking according to pre-strain: (a) 590DP; (b) 980DP

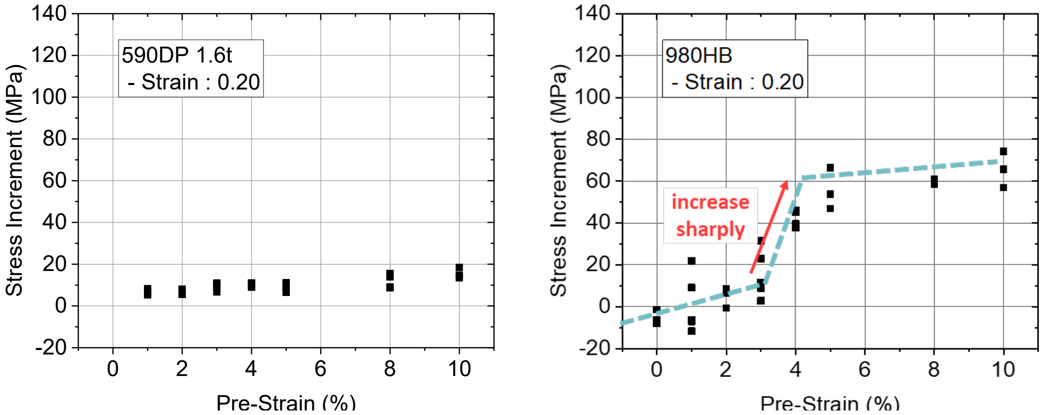

(a) (b)

Fig.16: Variation of true stress increment with respect to the pre-strain at strain of 0.2 after baking according to pre-strain: (a) 590DP; (b) 980DP

The engineering stress-strain curves in Fig. 6 were converted to the true stress-strain curves in Fig. 15 using the DIC inverse method. 590DP steel, in which no yield point elongation occurs has a similar shape to the stress-strain curve of original material after baking. The slope of the stress-strain curve gradually decreases until near the uniform elongation, but after the uniform elongation, it becomes almost a straight line. On the other hand, 980DP shows yield point elongation in tensile test after baking. Therefore, the stress in the stress-strain curve sharply decreases after the upper yield point and then increases again. Like 590DP steel, 980DP steel also has an almost straight stress-strain curve after uniform elongation, but the strength increase is significantly greater than that of 590DP steel. Fig. 16 shows the increase in strength compared to the original at a strain rate of 0.2. 590DP has a stress increase of less than 20 MPa. The material strength of 980DP increases gradually up to 3% of the pre-strain, but increases rapidly up to 5% and then increases to about 70MPa.

4 Simulation method considering both forming and baking

4.1 Work hardening model to describe effects of baking according to pre-strain

In order to apply the stress-strain curve in Fig. 15 into simulation as material properties, a work hardening model is required. Therefore, this study proposes a mathematical work hardening model.
The material strength variation after baking can be divided into a drastic decrease after the peak stress in yield point elongation and an increase in the overall work hardening curve as shown in Fig. 17.
As shown in Fig. 16(b), the work hardening curve has a transition zone of 3~5% pre-strain in which the strength increases rapidly. it is classified into the work hardening curve of the original material (σ_{AR}), the increase in the work hardening curve by baking ($\Delta\sigma_{Shift}$), and the increase in initial stress by yield point elongation ($\Delta\sigma_{Peak}$), as shown in Fig. 18, and is expressed as in equation (12).

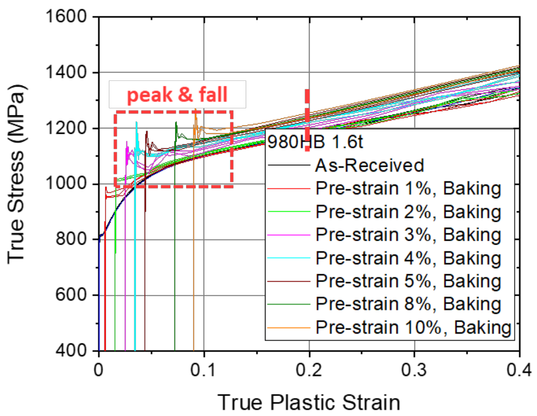

Fig.17: Analysis of stress variation with respect to the pre-strain

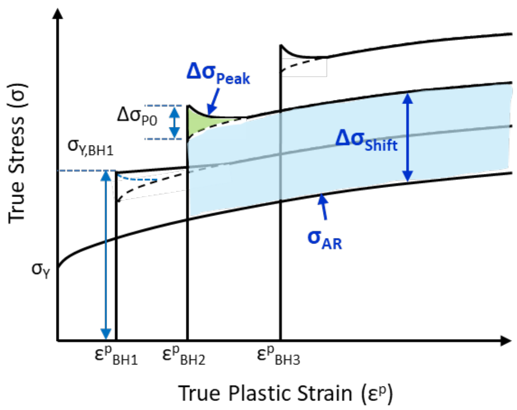

Fig.18: Classification of stress in stress-strain curve after pre-strain and baking

$$\sigma = \sigma_{AR} + \Delta\sigma_{Shift} + \Delta\sigma_{Peak} \tag{12}$$

590DP and 980DP steels were fitted by the new work hardening model and compared with the experiment as shown in Fig.19. Both 590DP without yield point elongation and 980DP with yield point elongation were well described by the new work hardening model.

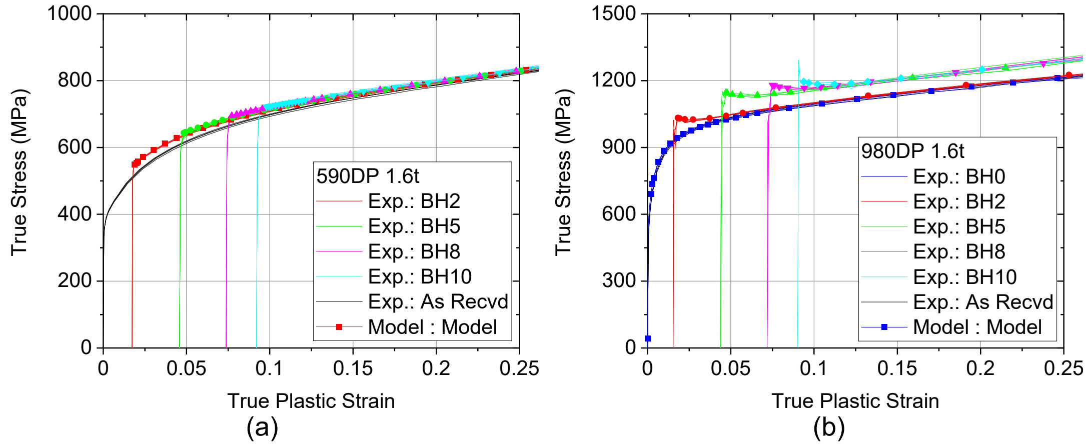

Fig.19: Comparison of new hardening model for BH and experiment: (a) 590DP; (b) 980DP

4.2 Validation of new model using LS-Dyna user material subroutine

The newly proposed work hardening model considering pre-deformation and baking was constructed and verified as LS-Dyna user material subroutine. As the first benchmark test, simple tension was performed with quarter model in Fig. 20. If the pre-strain is not constant in the longitudinal direction, necking happens at the beginning of the tension, and it is difficult to verify the baking effect. Therefore, the pre-strain was constant in the longitudinal direction, and pre-strain of 0.01 and 0.05 were applied the top and bottom, respectively. Fig. 21 shows the stress-strain curves by the new work hardening model of 590DP for pre-strain of 0, 0.01, 0.03, 0.05, and 0.1 used in the benchmark test.

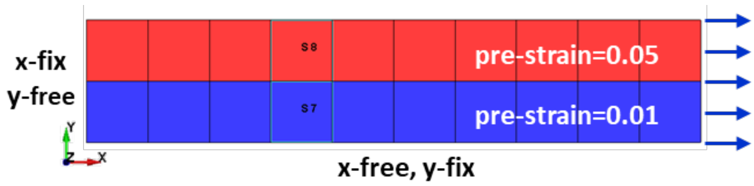

Fig.20: FE model of benchmark test for simple tension

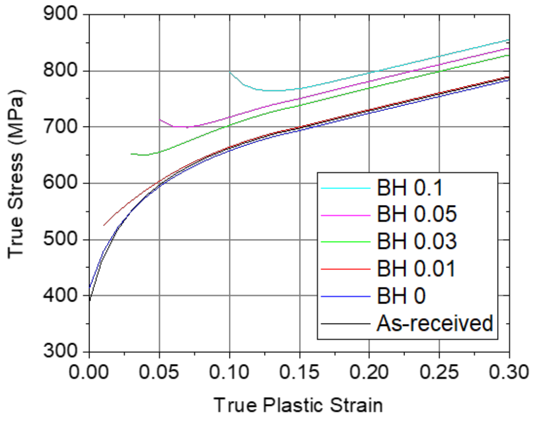

Fig.21: Stress-strain curves of 590DP steel from new model for BH

When the test model is tensioned with uniform velocity in the x-direction, the stress and strain of elements 7 and 8 were measured and compared with input material properties. As a result of the analysis, it was confirmed that input stress-strain curve and simulation matched exactly as shown in Fig. 22, thereby verifying that the user material subroutine was constructed well.

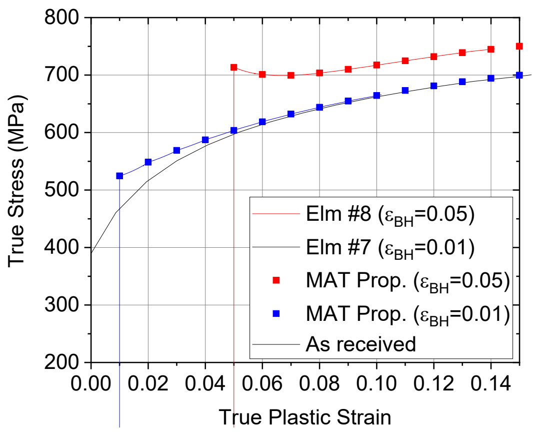

Fig.22: Comparison of stress-strain curves of simulation with input hardening model

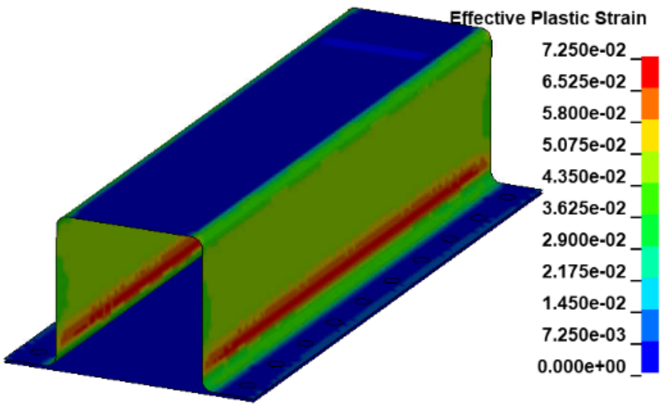

Fig.23: Contour of pre-strain in single hat specimen

In order to confirm the effect of strength increase by forming and baking, the simulation of axial crush of a hat specimen in Fig. 23 was performed. The thickness reduction on the wall by about 5% generated by forming simulation. The spot weld fracture was not considered. One side was fixed and the other side was collapsed vertically at constant velocity. Compared to the original material, the case that considered both work hardening and bake hardening, showed the greatest load and energy absorption. The energy absorption of the case considering both work hardening and bake hardening approximately 5% larger that that of case considering only work hardenging. This difference is significant level in crash performance. Therefore, it is necessary to apply the bake hardening according to the pre-strain as well as work hardening in order to accurately predict the crashworthiness.

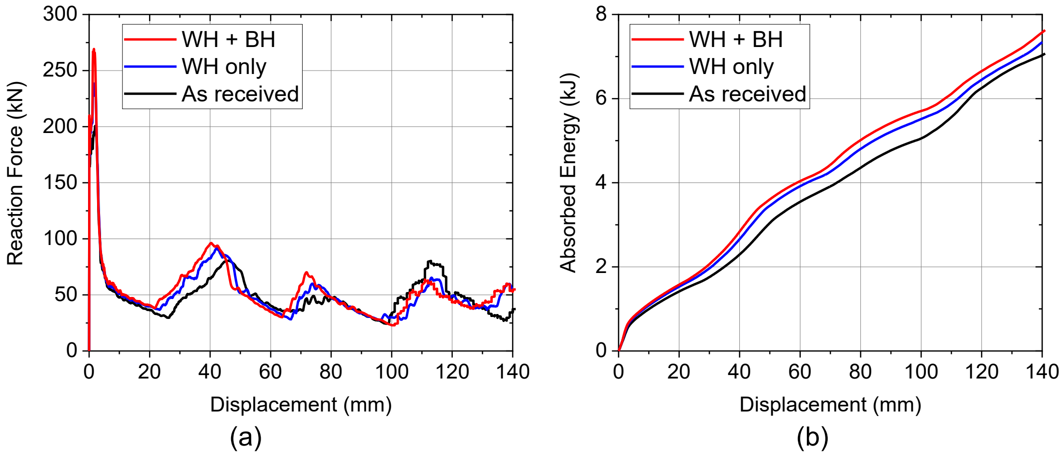

Fig.24: Effects of consideration of work hardening and bake hardening in the axial crash of single hat specimen on: (a) force-displacement curve ;(b) absorbed energy

5 Summary

A test method and work hardening model were developed to consider the material properties that change due to pre-deformation by forming and bake hardening in the painting process, in the collision analysis. In order to prevent the fracture in the curvature of a tensile specimen caused by the difference in bake hardening due to the non-uniform pre-strain, the tensile specimen was re-machined from the parallel section of a large specimen to which the pre-strain was applied, and re-tensioned it. The strain measured by the DIC system in the deformed specimen was converted into the strain before pre-deformation. When baking after pre-deformation, giga-steel usually shows the yield point elongation, and the upper yield point reaches the tensile strength as pre-strain increases. Therefore, it is impossible to calculate the stress-strain curve numerically. In this study, it was developed the DIC inverse method that obtains the stress-strain curve by comparing the force calculated from the strain measured by DIC system with force-displacement curve from a test. Stress-strain curves of 590DP and 980DP steels were derived using the DIC inverse method. Novel work hardening model was developed to apply the change in the stress-strain curve according to pre-strain and baking into simulation. The model is expressed as the sum of the terms for the work hardening curve of the original material, the strength increase due to baking, and the increase in initial stress due to yield point elongation. In order to apply the new work hardening model to the simulation, an LS-Dyna user material subroutine was constructed and verified by a benchmark test of a simple tensile specimen. In the axial crush of a hat specimen, considering both work hardening and bake hardening showed a significant difference in crash performance compared to only considering work hardening. Therefore, it is necessary to consider bake hardening according to forming history for accurate prediction of the crash analysis.

6 Literature

[1] T.B. Stoughton, J.W. Yoon, J.Y. Min, J.E. Carsley, A DIC Technological Revolution, in: Proc. FTF Conference, 2019
[2] D. Koch, F. Andrade, A. Haufe and M. Feucht, Bake-Hardening Effect in Dual-Phase Steels Experimental and Numerical Investigation, 15th International LS-DYNA Users Conference, 2018
[3] D. Riemensperger(Opel), Considering Bake Hardening for Deformed Sheet Steel, German LS-DYNA Forum 2016
[4] S. Thuillier , S.L. Zang, J. Troufflard, P.Y. Manach and A. Jegat, Modeling Bake Hardening Effects in Steel Sheets-Application to Dent Resistance, Metals, 8, 594, 2018
[5] R. Schwab and V. Ruff, On the nature of the yield point phenomenon, Acta Materialia 61, 1798-1808, 2013

[6] V. Ballarin, M. Soler, A. Perlade, X. Lemoine, and S. Forest, Mechanisms and Modeling of Bake-Hardening Steels: Part I. Uniaxial Tension, METALLURGICAL AND MATERIALS TRANSACTIONS A, VOLUME 40A, 1367-1374, 2009
[7] L. Durrenbergera, X. Lemoinea and A. Molinari, Effects of pre-strain and bake-hardening on the crash properties of a top-hat section, Journal of Materials Processing Technology, 211, 1937-1947, 2011